# Enhancement of near-inertial waves by cyclonic eddy in

# the northwestern South China Sea during spring 2022

- 3 Qi'an Chen<sup>1,2</sup>, Hongzhou Xu<sup>1\*</sup>, Dongxiao Wang<sup>3,4</sup>, Bo Hong<sup>5\*</sup>, Chunlei Liu<sup>6,7,8</sup>,
- 4 Zheyang Zhang<sup>1</sup>, Huichang Jiang<sup>1</sup>, Wei Song<sup>3</sup>, Tong Long<sup>1</sup>, Ling Wang<sup>1,2</sup>, Sumin Liu<sup>1</sup>,
- 5 Rongjie Chen<sup>1,2</sup>
- 6 <sup>1</sup>Institute of Deep-sea Science and Engineering, Chinese Academy of Sciences, Sanya, 572000, China
- 7 <sup>2</sup>University of Chinese Academy of Sciences, Beijing, 100049, China
- 8 <sup>3</sup>School of Marine Sciences, Sun Yat-sen University, Zhuhai, 519000, China
- 9 <sup>4</sup>South Marine Science and Engineering Guangdong Laboratory (Zhuhai), Zhuhai, 519082, China
- 10 <sup>5</sup>School of Civil and Transportation Engineering, South China University of Technology, Guangzhou,
- 11 510641, China
- 12 <sup>6</sup>College of Ocean and Meteorology, Guangdong Ocean University, Zhanjiang, 524088, China
- 13 <sup>7</sup>South China Sea Institute of Marine Meteorology, Guangdong Ocean University, 529568, Zhanjiang,
- 14 China
- 15 8CMA-GDOU Joint Laboratory for Marine Meteorology, Guangdong Ocean University, Zhanjiang,
- 16 524088, China
- 17 Correspondence to: Hongzhou Xu (Email: hzxu@idsse.ac.cn); Bo Hong (bohong@scut.edu.cn)
- 18 Abstract. By analyzing dataset derived from four moorings during spring 2022, this study provides
- 19 direct evidence that near-inertial waves (NIWs) can be largely enhanced by a passing cyclonic eddy
- 20 (CE) in the northwestern South China Sea. Results show that the enhancement of NIWs mainly
- 21 occurred at north side of the CE due to asymmetry of eddy structure. In vertical, the enhancement
- 22 concentrated at above 200 m and reached peaks at around 100 m. Significant energy transfer rates
- between the CE and NIWs appeared at the same depth of the enhancement can reach up to  $6 \times 10^{-10}$
- 24 m<sup>2</sup>/s<sup>3</sup> at the CE's edge Under the impact of the CE, power of the first five NIWs modes was promoted
- 25 significantly and dominated by the second and third modes. Overall, the CE transferred energy to
- 26 NIWs before near-inertial kinetic energy reaching its peaks, while NIWs gave energy back to the CE
- after the peaks.

28

# 1 Introduction

- Near-inertial waves (NIWs) are ubiquitous features throughout the global ocean with frequencies
- 30 near the Coriolis frequency f (Garrett, 2001). As dominant modes of high-frequency variability in
- 31 oceans, they contain half of the kinetic energy in internal wave fields (Alford, 2003; Alford et al., 2016;

删除: that

删除:,

删除: with an energy transfer efficiency  $(\epsilon/W)$  of approximately 25%.

删除: impact

删除: were

32 Ferrari and Wunsch, 2009). NIWs transfer energy from mixed layer to interior and ultimately dissipate 33 into microscale turbulence, providing an energy source for abyssal diapycnal mixing (Chen et al., 2017; Ferrari and Wunsch, 2009). Therefore, NIWs are of vital importance for energy cascade among 34 35 multiscale dynamic processes. 36 Due to horizontal spatial scales of 10-100 km and slow group speed of NIWs, they are likely to 37 interact strongly with mesoscale eddy in oceans (Alford et al., 2016). Besides resonant frequency 38 shifting from local f to the effective inertial frequency caused by mesoscale vorticity (Klein et al., 2003; 39 Kunze, 1985; Weller, 1982), energy exchange between eddy and NIWs also plays an important role in 40 oceanic energy cascade (Ferrari and Wunsch, 2009; Thomas, 2017). Researchers have stated that the 41 NIWs can extract energy from eddy and affect the vertical material transport (Barkan et al., 2021; 42 Esposito et al., 2023). Moreover, energy transfer from mean flows can balance the dissipation of near-43 inertial energy near the critical layer, thereby conserving near-inertial energy during eddy migration, 44 (Xu et al., 2022b). 45 Jing et al. (2017) and Jing et al. (2018) suggested that there is a permanent energy transfer from 46 eddies to NIWs under a positive Okubo-Weiss parameter condition. Furthermore, Yu et al. (2022) 47 revealed that enhanced near-inertial kinetic energy (NIKE) is found preferentially in regions of 48 anticyclonic vorticity. Using surface drifter dataset, Liu et al. (2023) indicated that bidirectional energy 49 transfer exists between eddy and NIWs in the global oceans. Above studies all emphasized role of eddy 50 on affecting frequencies of NIWs, NIKE as well, 51 As the largest semi-enclosed marginal sea in the northwestern Pacific Ocean, the South China Sea

52

53

54

55

56

57

58

59

60

61

删除: t mixing

删除: transfer

删除: Moreover, enhanced wave dissipation near the critical layer balances the energy transfer from mean flows and conserve the near-inertial energy during eddy migration

删除: can be transferred

# 删除:

删除: As the largest semi-enclosed marginal sea in the northwestern Pacific Ocean, the South China Sea (SCS) has frequent eddy activities (Chen et al., 2011; Chu et al., 2014; Nan et al., 2011; Wang et al., 2008; Wang et al., 2003). Using different eddy detection algorithms and criteria, many studies have statistically investigated the eddy number and mean properties (Lin et al., 2007; Wang et al., 2003; Xiu et al., 2010) Chen et al. (2011) suggest that eddies present 35%-60% of the time in the northern SCS, which play an important role in material transport and energy transfer (He et al., 2018; Liu et al., 2023; Zhang et al., 2015; Zhang et al., 2023; Zhang et al., 2019). Researchers have examined eddy properties (Wang et al., 2023; Zhao et al., 2023), eddy structures (Chu et al., 2022; He et al., 2018; Zhang et al., 2016) and energy exchange during eddy process in the northern SCS (Chu et al., 2014; Fan et al., 2024; Huang et al., 2018; Liu et al., 2023; Xu et al., 2022a; Zhang et al., 2023).

(SCS) has frequent eddy activities (Wang et al., 2003; Wang et al., 2008; Chen et al., 2011; Nan et al.,

2011; Chu et al., 2014). Early studies, by using various eddy detection algorithms, have statistically

characterized the mean properties of eddies, identifying peak occurrences along western boundary

currents and shelf break regions (Wang et al., 2003; Lin et al., 2007; Xiu et al., 2010). Specifically,

Chen et al. (2011) indicated that eddies occur 35%-60% of the time in the northern SCS, underscoring

their critical role in regional oceanography. Recent advancements in remote sensing and in-situ

observational technologies have enabled significant insights into eddy formation and their three-

dimensional structures (Nan et al., 2011; Zhang et al., 2016; He et al., 2018; Chu et al., 2022; Wang et

al., 2023). Due to their unique three-dimensional structures and spatiotemporal scales, eddies mediate

significant material transport (Zhang et al., 2015; He et al., 2018; Zhang et al., 2019) and substantial

energy exchanges with internal waves and western boundary currents (Chu et al., 2014; Huang et al., 2018; Xu et al., 2022; Liu et al., 2023; Zhang et al., 2023; Zhao et al., 2023; Fan et al., 2024),

In the northwestern SCS, large portion of eddy propagate westward and terminate near Xisha Trough (Fig. 1a(Wang et al., 2003; Zhai et al., 2010), making this place as an ideal area for investigating NIWs and its interaction with eddy. However, interaction and energy exchange processes between them remain to be investigated in this area. In this study, four moorings, each equipped with a Teledyne RD Acoustic Doppler Current Profiler (ADCP), were deployed in the Xisha Trough of the northwestern SCS (Fig. 1a). During spring 2022, a cyclonic eddy (CE) propagated westward across the mooring array, giving an opportunity to study energy transfer between NIWs and the CE in this area. We introduce data and methods in Section 2, present the observation results in Section 3, discuss energy transfer between NIWs and the CE in Section 4, and give a conclusion in Section 5.

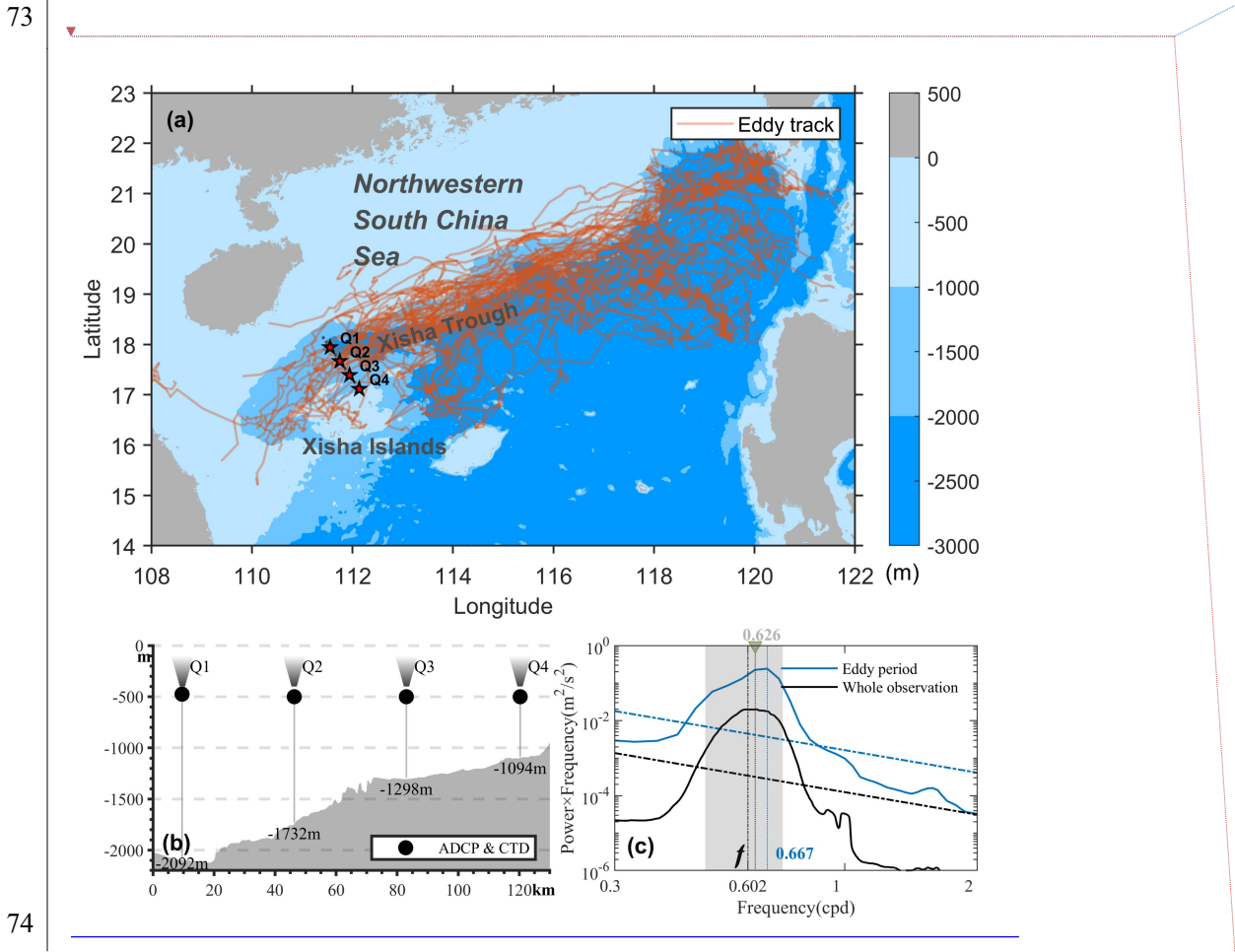


**Figure 1: (a)** Location of four moorings (Q1-Q4) in the northwestern SCS. The shaded background color represents topography. Orange lines indicate tracks of long-lasting eddy propagating from the Luzon area to the Xisha Trough from 1993 to 2023. **(b)** Structure of upward-looking ADCP mooring along the slope of topography. **(c)** The power spectra during eddy period (blue line) and whole observation period (black line). The spectra are

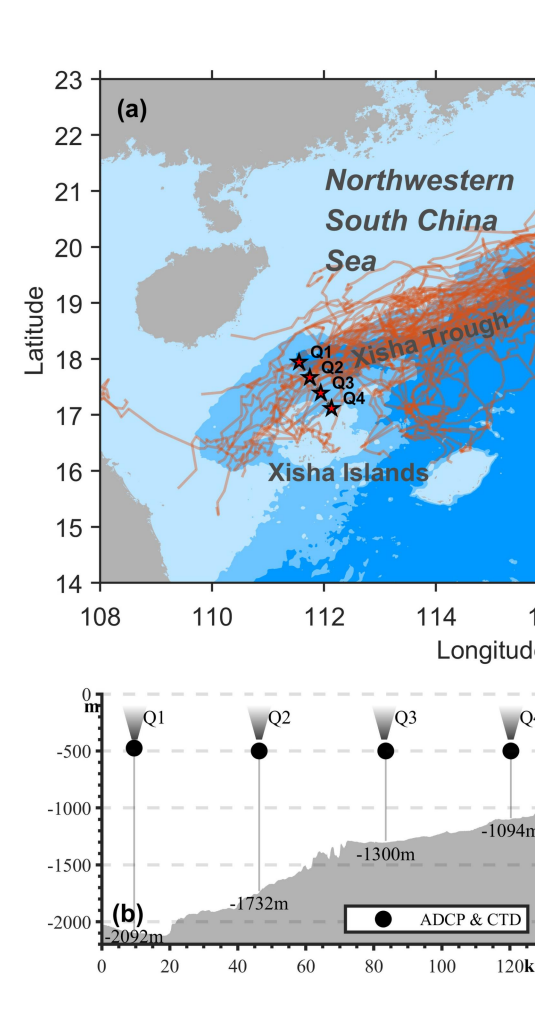
删除: As the largest semi-enclosed marginal sea in the northwestern Pacific Ocean, the South China Sea (SCS) has frequent eddy activities (Chen et al., 2011; Chu et al., 2014; Nan et al., 2011; Wang et al., 2008; Wang et al., 2003). Early studies, leveraging various eddy detection algorithms, hav

删除: a

删除: seemly

删除: instrument

删除: observing



删除:

删除:

# 2 Methodology

#### 2.1 Data

79

80

81

91

92

93

94

95

96

97

98

99

100

The four moorings (Q1-Q4) were deployed in the study area on August 21-23, 2021. One upward-82 looking 75-kHz ADCP along with a CTD (SBE 37sm) was fixed at approximately 480 m depth and 83 84 continuously monitored current velocity for each mooring (Fig. 1b). The ADCPs were set to have 30 85 bins with 16 m of vertical interval and 30 minutes of temporal interval, enabling extraction of NIWs of 86 the upper ocean. The moorings were recovered on November 13-15, 2022. Several ADCP bins near the sea surface were omitted due to large fluctuations, and the remaining were vertically linearly 87 88 interpolated to 1m resolution. Due to the significant vertical fluctuations based on CTD data in certain 89 periods, flow velocity compensation correction was applied to ADCP data, which was calculated based 90 on depth change and flow direction.

The Copernicus Marine Environment Monitoring Service (CMEMS) provides daily geostrophic current and sea level anomaly (SLA) data with a resolution of  $0.25^{\circ} \times 0.25^{\circ}$ , which were used to detect eddy during the observation period. The  $1/12^{\circ}$  three-dimensional products were obtained from CMEMS to calculate energy transfer rate between eddy and NIWs. The eddy dataset from Archiving, Validation, and Interpretation of Satellite Oceanographic (AVISO) was used to provide the trajectories and edges of the eddy. World Ocean Atlas (WOA18) data was used to extract temperature and salinity data. The European Centre for Medium-Range Weather Forecasts (ECMWF) Reanalysis V5 (ERA-5) data, which has hourly temporal and  $0.25^{\circ}$  spatial resolutions, was used to calculate near-inertial energy input from the wind field.

#### 2.2 Method

The method for ADCP velocity flow velocity compensation correction is as follows:

102 
$$\vec{V}_{\underline{\text{true}}}(t) = \vec{V}_{\underline{\text{measured}}}(t) + \vec{V}_{\underline{\text{platform}}}(t),$$
 (1)

103 
$$\vec{V}_{\text{platform}}(t) = \frac{\Delta x}{\Delta t} \vec{i} \pm \frac{\Delta y}{\Delta t} \vec{i}$$
 (2)

104 
$$(x,y) = (\rho\cos\theta, \rho\sin\theta),$$
 (3)

删除:

删除: vertically

删除: observing

删除: SLA

删除: validate the existence of eddy and

删除: y

删除: eddy's center



#### 3 Results

132

133

134

135

136

137

138

139

140

141

142 143

144

145

146

147

# 3.1 Near inertial frequency and NIKE

删除:

The snapshots of SLA and surface geostrophic velocity fields show that the CE approached the mooring array on February 1 (Fig. 2). Its center passed through Q3 around February 26 and it left the mooring array on March 9. During the entire observation period, NIWs exhibit a small blue shift of 删除: whole near-inertial frequency with a peak value of 0.616 cycles per day (cpd) (Fig. 1c), while a significant 删除: have blue shift occurred during the eddy period (February 1 - March 9) due to the background positive 删除: . vorticity of the CE. The peak of spectral frequency  $(\omega_p)$  reached 0.667cpd, with a relative frequency 删除: W shift  $(\frac{\omega_p - f}{f}, RFS)$  of about 10.8% in this area. It is significantly larger than the global RFS (Guo et al., 删除: appeared

2021), suggesting significant impact of the CE on local near-inertial frequencies.

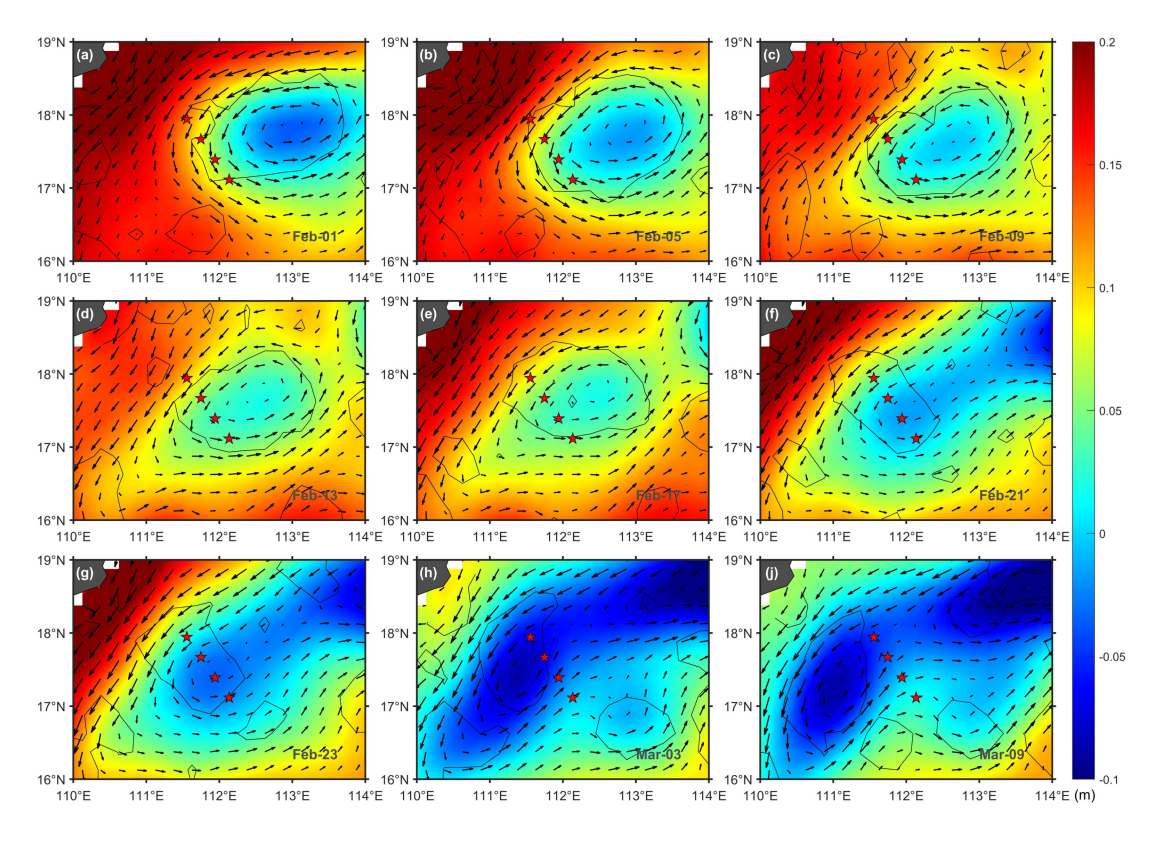


Figure 2: (a-j) The snapshot of sea level anomaly and geostrophic current vector during February 1-March 9. The black line indicates the Okubo-Weiss parameters.

Meridional velocity wavelet power spectra show that strong power of NIWs occurred during eddy period but with large variations at different eddy stages (Figs. 3a-d). To quantify NIKE at different 删除: qualify stages of the CE, we defined two time periods named as Period1 (February 16-26) and Period2

(February 26-March 8), covering 10 days before and after the eddy's center passed through the mooring array. In addition, no eddy period with calm wind during June 1-20 was chosen for extra comparison. Figs. 3e-h show temporal and vertical variations of NIKE at the four moorings during eddy period. The missing data of NIKE at surface layers are due to mooring swing caused by strong currents. It can be seen that NIKEs were enhanced largely at above 200 m during Period2. And peak values of NIKE concentrated at around 100 m. The time-averaged NIKEs during Period2 have almost one order larger than that during no eddy period (Figs. 3i-1), suggesting significant impact of the CE on local NIKE. Moreover, NIKEs illustrate asymmetry in space during eddy period (Figs. 3e-1). At north side of the CE (Q1-Q2), NIKEs became much stronger than that at south side of the CE (Q3 and Q4), especially at Q2 with a maximum value up to 12.0 J/m³ (Fig. 3f), which has the same magnitude as the result observed by Xu et al. (2022b).

删除: absences

删除: spatial

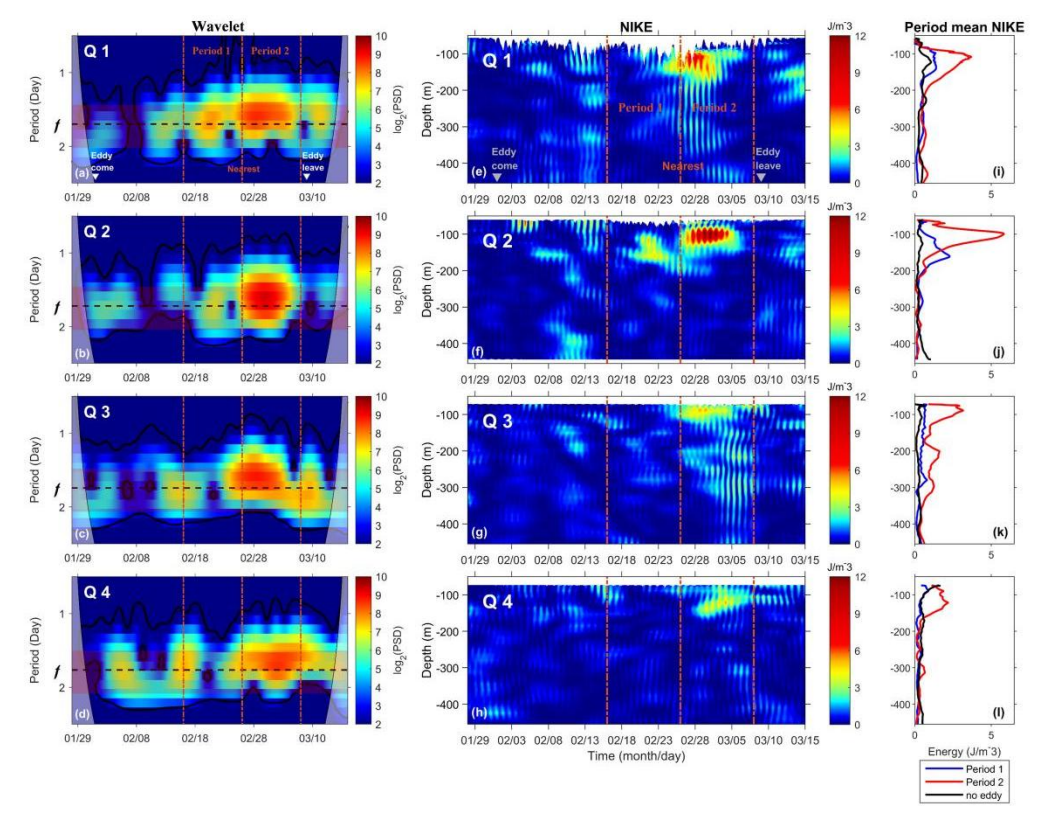


**Figure 3: (a-d)** 100 m-depth meridional velocity wavelet power spectra at Q1-Q4 during eddy period. **(e-h)** Vertical distribution of NIKE at Q1-Q4. The gray triangles indicate the time when the CE edge contacts and leaves the mooring array. **(i-l)** Vertical distribution of time-averaged NIKE during 'no eddy period' (black line), 'Period 1' (blue line), and 'Period 2' (red line) at Q1-Q4. The red dashed lines mark two periods of the CE.

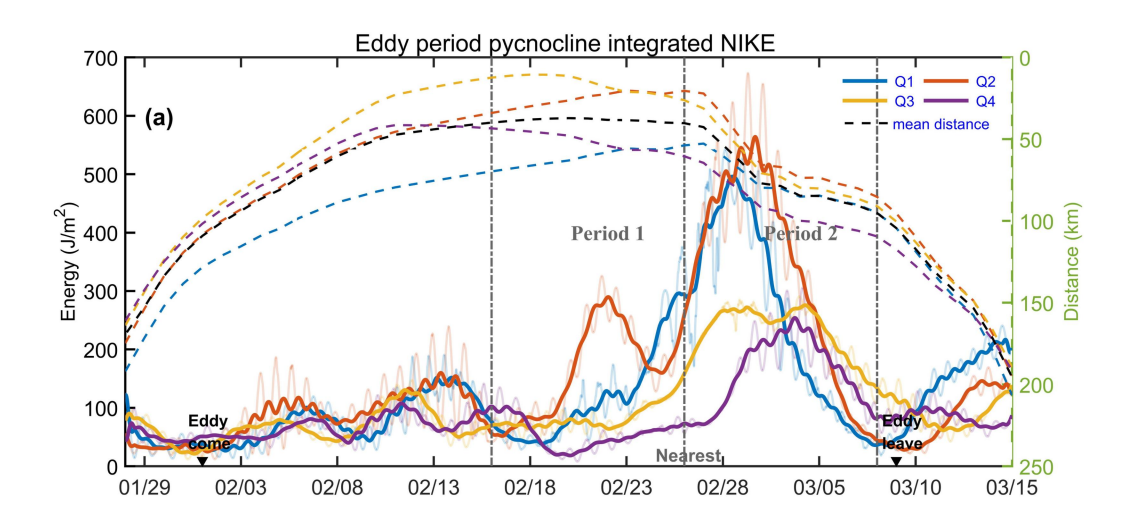
#### 3.2 Impact of eddy on NIWs

To ensure the fact that the CE could largely enhance NIWs in the northwestern SCS, we compared

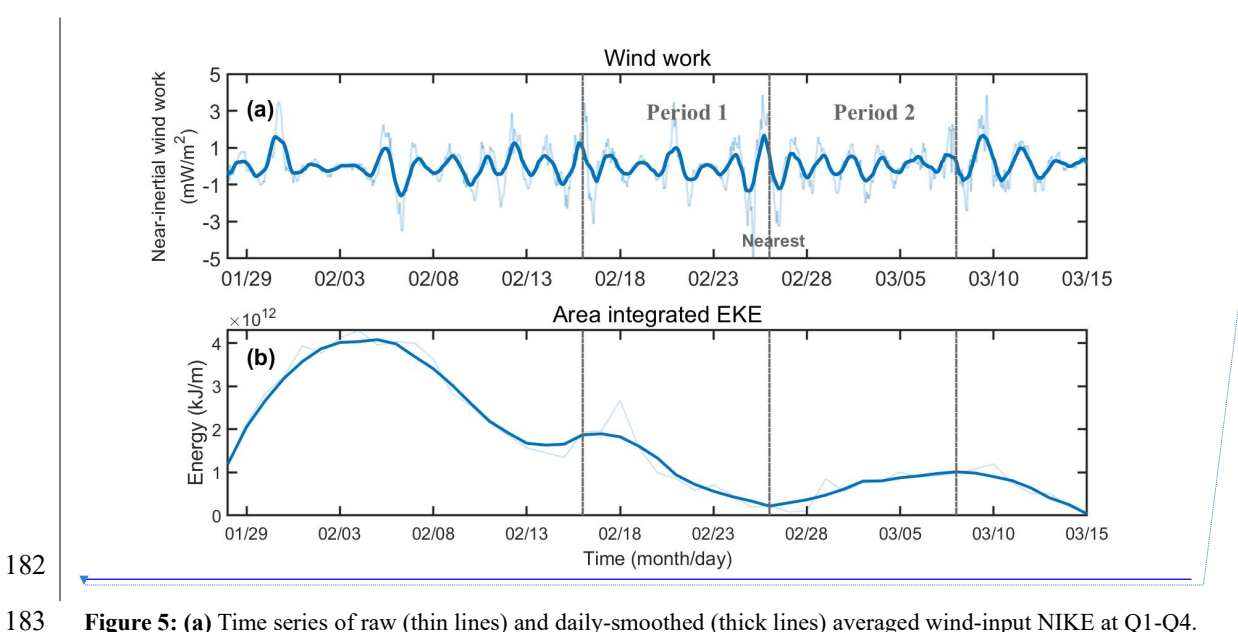
time series of vertical-integrated (above 200m) NIKE at each mooring with mooring-eddy distance, wind-input NIKE and eddy kinetic energy (EKE) in the study area (Fig. 4 and Fig. 5). NIWs were enhanced gradually accompanied by weakening EKE during Period1 when wind-input NIKE were relatively stable and minor. The percentage changes in the averages of NIKE and EKE for two time periods, before February 16th and from February 16th to March 8th, were 115.2% and -71.6%, respectively. Results suggest a vivid energy transfer from Eddy to NIWs during this period that will be quantified and discussed in Section 4. After passing of the CE's center, the CE enhanced NIWs faster, indicating more energy transfer from eddy to NIWs during Period2 than that during Period1. The slight increase of EKE during Period2 was contributed by background western boundary current velocity input (Fig. 2).

删除: Results suggest a vivid energy transfer from eddy to NIWs during this period that will be qualified quantified and discussed in Section 4.

删除: 1a

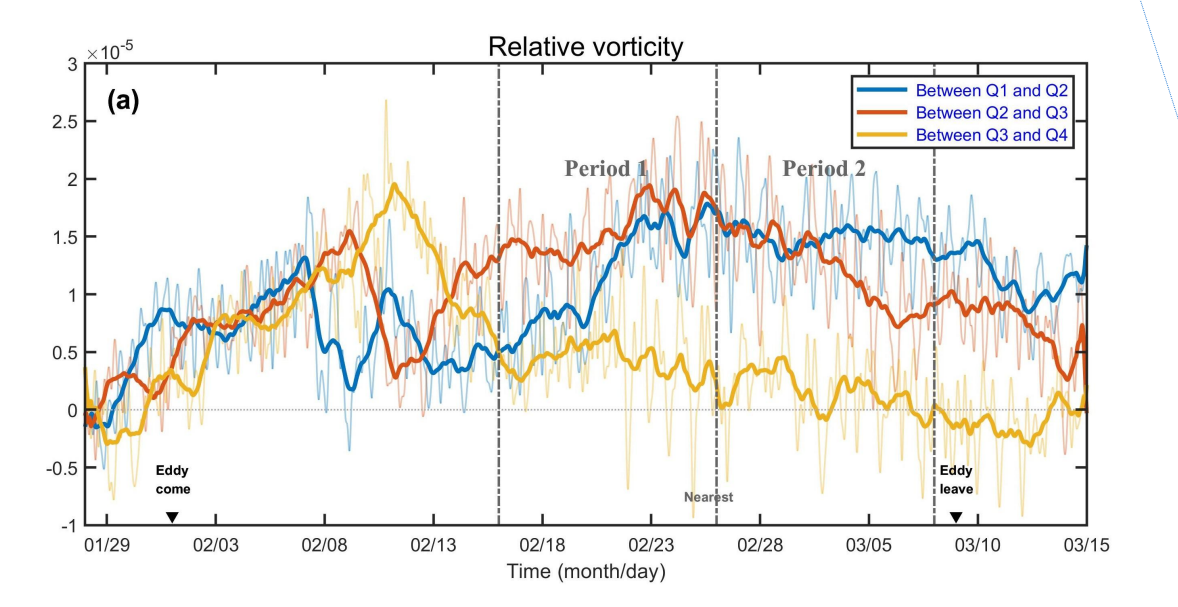


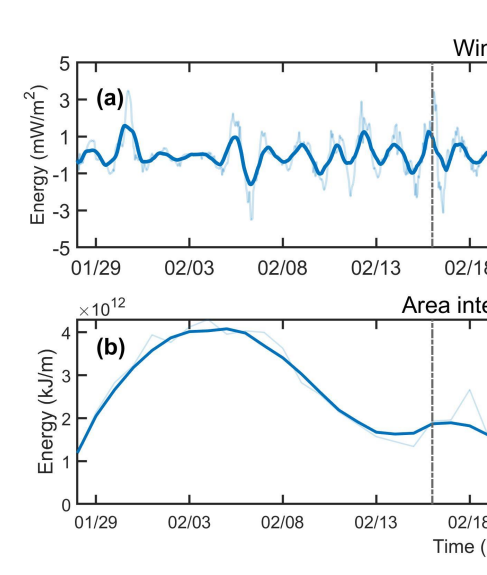
**Figure 4:** Time series of raw (thin lines) and daily-smoothed (thick lines) depth-integrated (above 200 m) NIKE at Q1-Q4 (solid lines) accompanying with distance between the CE's center and each mooring (dashed lines) during eddy period. The black dashed line represents the mean distance between the CE's center and four moorings. The triangles mark the time when the eddy edge contacts and leaves the mooring array.



**Figure 5: (a)** Time series of raw (thin lines) and daily-smoothed (thick lines) averaged wind-input NIKE at Q1-Q4. **(b)** Time series of raw (thin lines) and daily-smoothed (thick lines) area integrated EKE.

In space, NIWs intensity reached 600 J/m<sup>2</sup> at Q2, whereas values at Q3 and Q4 were approximately 300 J/m<sup>2</sup>. This difference may be associated with the CE's vorticity distribution, where relative vorticities observed north of the CE (between Q1-Q2) were notably stronger than those measured south of the CE (between Q3-Q4) (Fig. 6). Zhao et al. (2021) and Zhao et al. (2023) pointed out that NIWs generation is significantly influenced by the eddy structure in which eddy with stronger shears tend to generate more powerful NIWs. In our case, Fig. 2 shows that the north side of the CE exhibited spatial overlap with the western boundary current of the northwestern SCS (Fig. 2) where





删除: In spatial, intensity of NIWs reached  $600 \text{ J/m}^2$  at Q2, while they merely had  $300 \text{ J/m}^2$  at Q3 and Q4 due to vorticity asymmetry of the CE in which relative vorticities at north side (between Q1 and Q2) were much larger than those at south side (between Q3 and Q4) (Fig. 6).

删除:

删除: In our case, the north side of the CE exhibited spatial overlap with the western boundary current of the northwestern SCS (Fig. 2) where strong shear is generated and could have enhanced NIWs largely at this side according to Zhao et al. (2021, 2023)

删除: In our case, the north side of the CE was merged with the western boundary current of the northwestern SCS (Fig. 1a) that generated strong shear and enhanced NIWs largely at this side.

- Figure 6: Time series of raw (thin lines) and daily-smoothed (thick lines) relative vorticity among four moorings.
- 196 Vertical gray dashed lines mark two periods of the CE.

195

197

#### 3.3 Impact of eddy on near-inertial modes

198 The CE not only affected frequency and energy of NIWs, but also their modes in the study area. 199 Here, we calculated vertical-averaged energy (above 200 m) of the first five modes of near-inertial 200 velocity during eddy period (Figs. 7a-d). All five modes grew since Period1 and reached peak values at 201 Period2. But the CE has different influence on different modes with low modes (mainly the second and 202 third modes) being significantly enhanced, especially near the CE's center. Low modes rose from 46% 203 (Q2) and 54.4% (Q3) of total energy during Period1 to 87.6% (Q2) and 79.5% (Q3) during Period2, 204 respectively (Figs 7e-f). The first mode has longer vertical wavelength and propagates faster than other 205 modes that make it easy escape from eddy's influence (Chen et al., 2013). Overall, energy proportion of 206 the first five modes were promoted from 81.5%, 66.8%, 69%, and 78.5% during Period1 to 90.8%, 207 88.8%, 87.7%, 94% at Q1-Q4, respectively (Figs. 7e-f), In conclusion, the cyclonic eddy has a 208 prominent influence on different modes of NIWs, resulting in the intensification of lower-mode energy 209 within its core region, especially for modes 2 and 3.

删除: , suggesting prominent influence of eddy on near-inertial modes in the northwestern SCS.

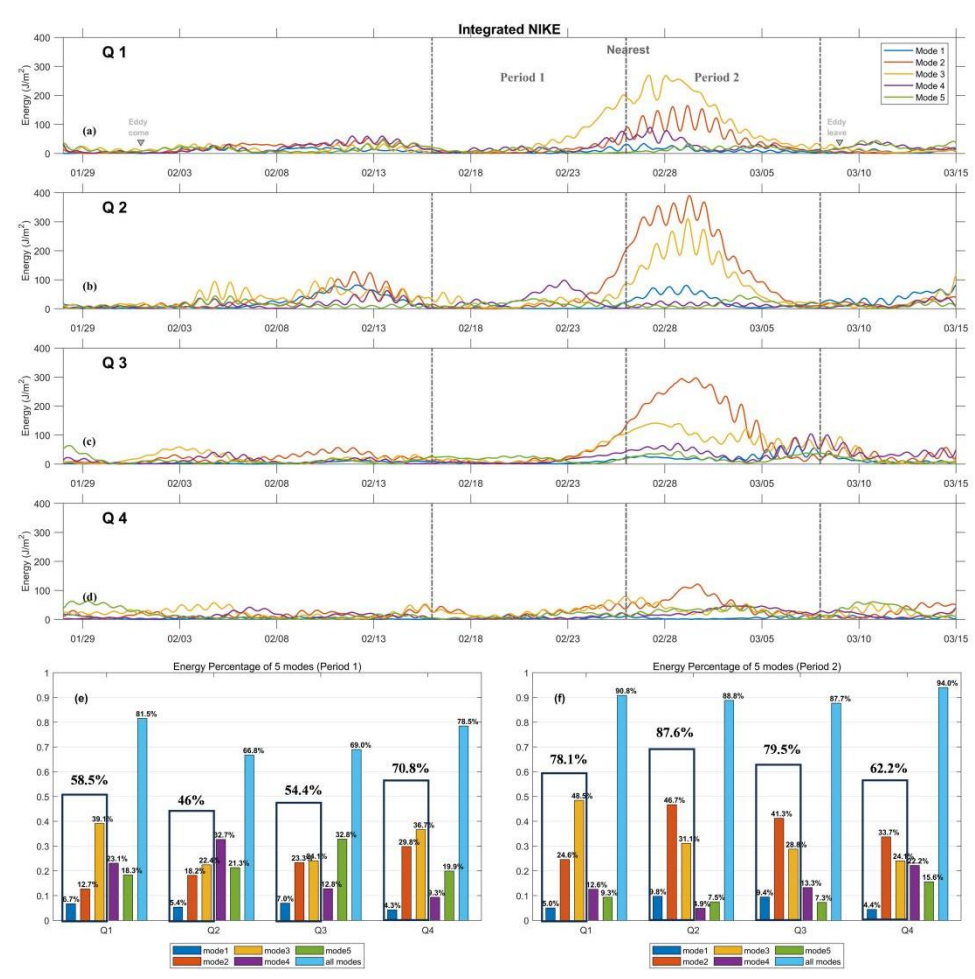


**Figure 7:** (a-d) Time series of NIKE for the first five modes at Q1-Q4 during eddy period. (e-f) The time-averaged proportions of each mode and all five modes during period 1 and period 2 at Q1-Q4. Black border indicates proportion sum of the first three modes.

# 4 Discussion

Energy exchange between eddy and NIWs is one of the most important processes in oceanic energy cascade (Alford et al., 2016; Ferrari and Wunsch, 2009; Thomas, 2017). By simulations, Jing et al. (2017) found that the energy transfer efficiency from eddies to near-inertial waves is about 2% of the near-inertial energy input by the wind in the Kuroshio Extension region. Based on surface drifter dataset, Liu et al. (2023) stated that energy transfer efficiency can reach about 13%, indicating previous underestimation of eddy impact on NIWs. For obtaining precise result, direct ocean current measurement by long-term mooring is essential (Jing et al., 2018). In this section, eddy-NIWs energy transfer rate during eddy period in the study area is qualified and discussed (Fig. 8). Corresponding to the layer of NIKE enhancement (Fig. 3), large energy transfer rates occurred at above 200 m with the peak values at around 100 m during eddy period, rather than surface and mixing layers (Jing et al.,

删除: By simulations, Jing et al. (2017) found that eddy-NIWs energy transfer efficiency is about 2% in Kuroshio Extension region

删除: was

225 2017; Liu et al., 2023). Both positive and negative transfer rates can reach a magnitude of 6×10<sup>-10</sup> m<sup>2</sup>/s<sup>3</sup> 226 in the study area, in which they are several times larger than the result of Jing et al. (2018) in the Gulf 227 of Mexico, but they are smaller than the result of Chen et al. (2023) in the Northwestern Pacific Ocean, 228 The differences may be attributed to the strength of eddies, their rotation direction and the intensity of 229 NIWs. Previous studies have shown that eddy rotation plays a critical role in energy transfer and NIWs 230 propagation due to differences in vorticity input and stratification modulation (Alford et al., 2016; Jing 231 et al., 2017). In addition, eddy-NIWs energy transfer is largely dependent on eddy structure in which 232 high rate can be caused by strong eddy shear (Zhao et al., 2023). It can be found that energy transfer at 233 Q1 and Q4 were more active than that Q3 due to occurrence of large shear strain at CE's edge (Figs. 234 9a-9b). Although NIKEs at Q4 were relative weak, the strong shear strains of the low frequency flow 235 promoted local transfer rates at this area, Thomas and Daniel (2020) and Li et al. (2022) both stated 236 that NIWs draw energy from the background flow when the energy ratio between them is small, and 237 vice versa. Similarly, our results show that positive/negative energy transfers from the CE to NIWs 238 dominated 'Before Strongest'/'After Strongest' periods at most mooring stations (Fig. 9c), indicating 239 an inhomogeneous and bidirectional energy transfer between eddy and NIWs during different periods 240 in the northwestern SCS.

删除:, but they are smaller than Chen et al. (2023)'s result.

删除: It can be found that energy transfer at the CE's edge (Q1 and Q4) was more active than at the CE's center (Q3). The higher energy transfer rate at Q1 generated stronger NIWs in this region, whereas Q4 exhibited a paradoxical pattern with strong transfer rates yet relatively weak NIKE. This discrepancy arises because the strong low-frequency flow strains (Figs. 9a–b) promoted the energy transfer rate but the net energy transfer rate remained low (Figs. 9c), resulting in weaker NIKE at Q4.

删除: It can be found that energy transfer at the CE's edge (Q1 and Q4) was more active than that at the CE's center (Q3). Although NIWs at Q4 were relative weak, the strong strains of the low frequency flow promoted local transfer rates at this area (Figs. 9a-b).

删除: NIWS draw energy from background flow with small energy ratio between them, vice versa

删除: (Alford et al., 2012; Furuichi et al., 2008; Zhai et al., 2009)

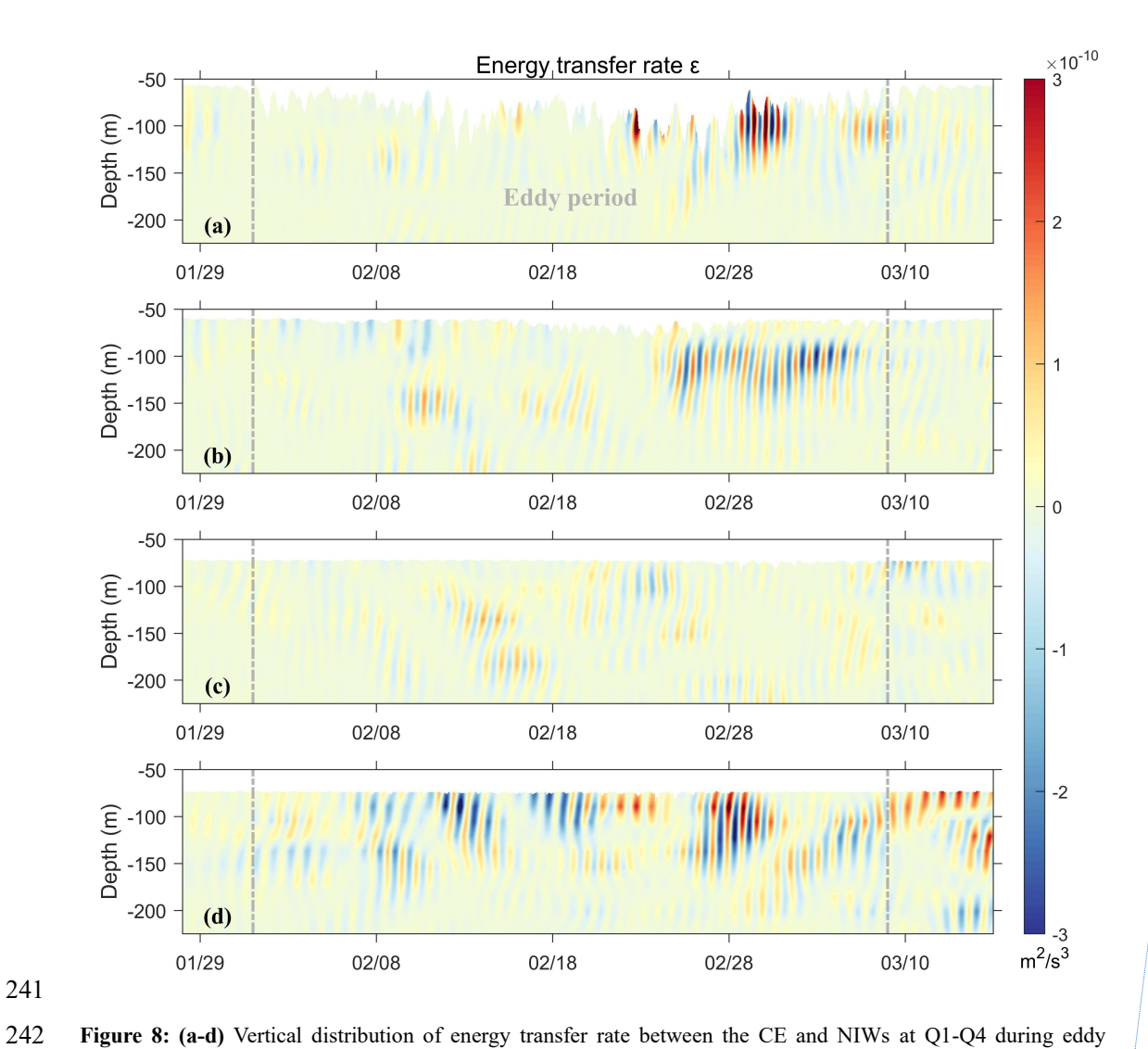
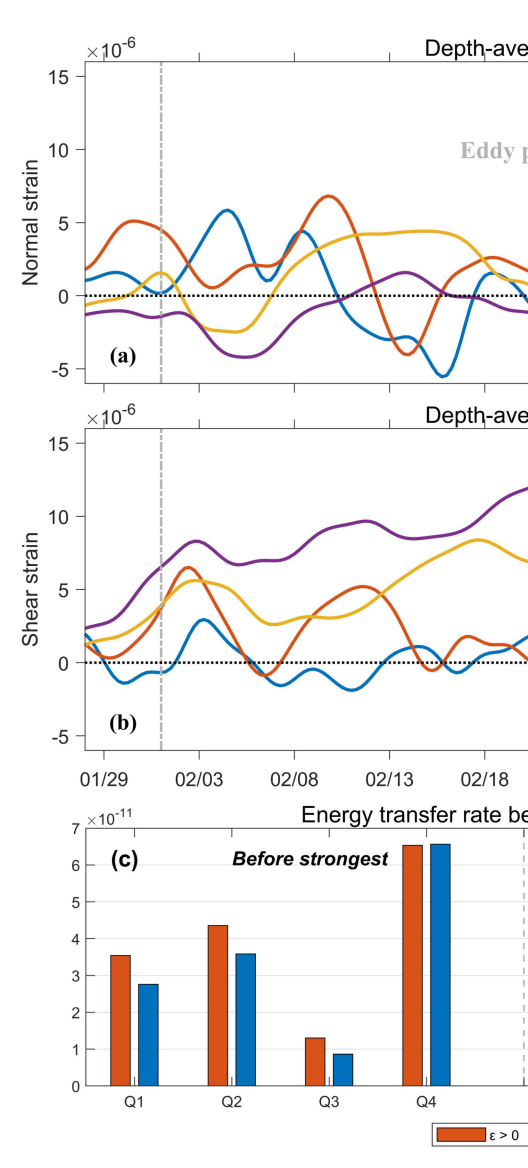


Figure 8: (a-d) Vertical distribution of energy transfer rate between the CE and NIWs at Q1-Q4 during eddy period.

244245

243



删除:

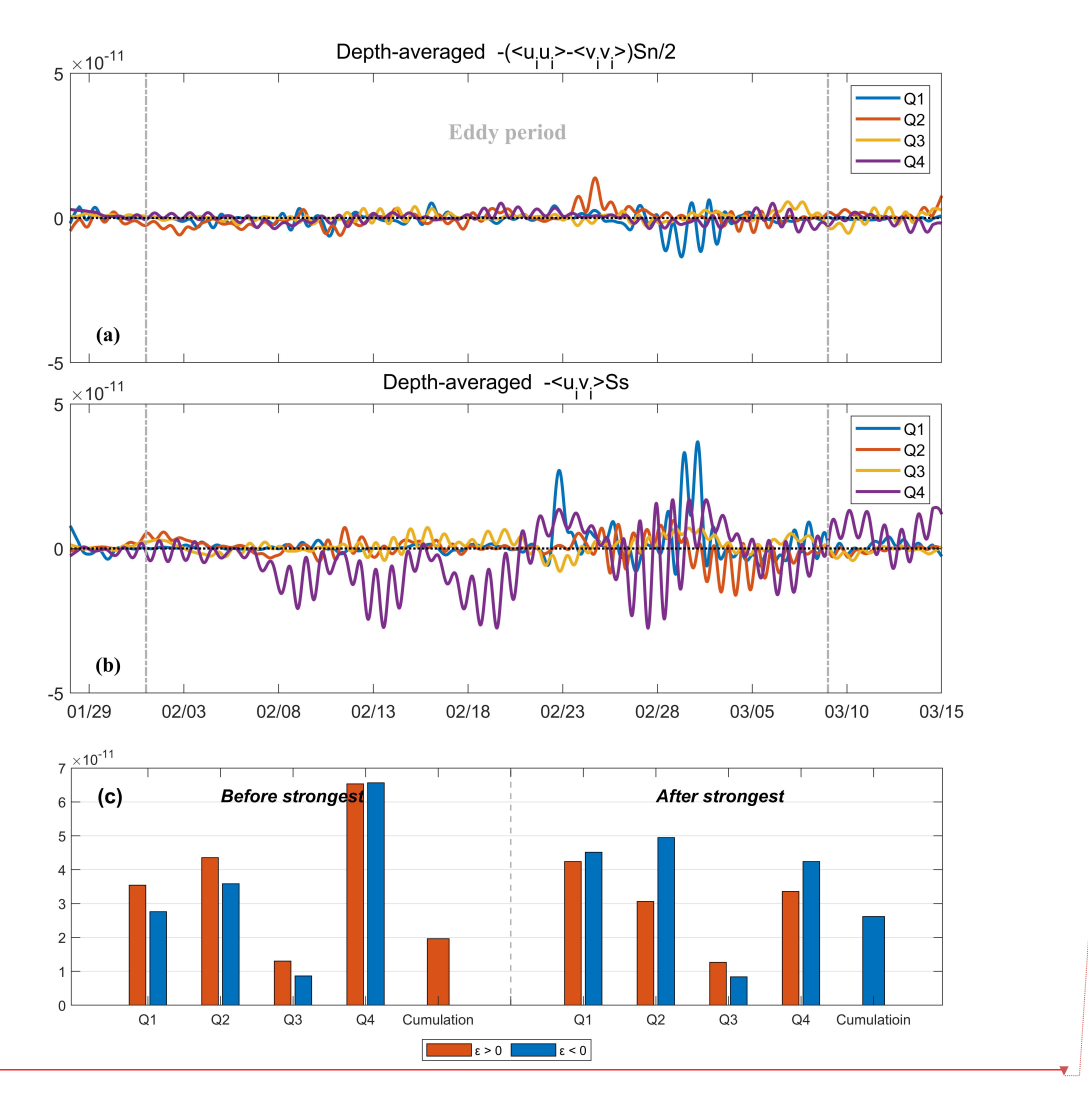
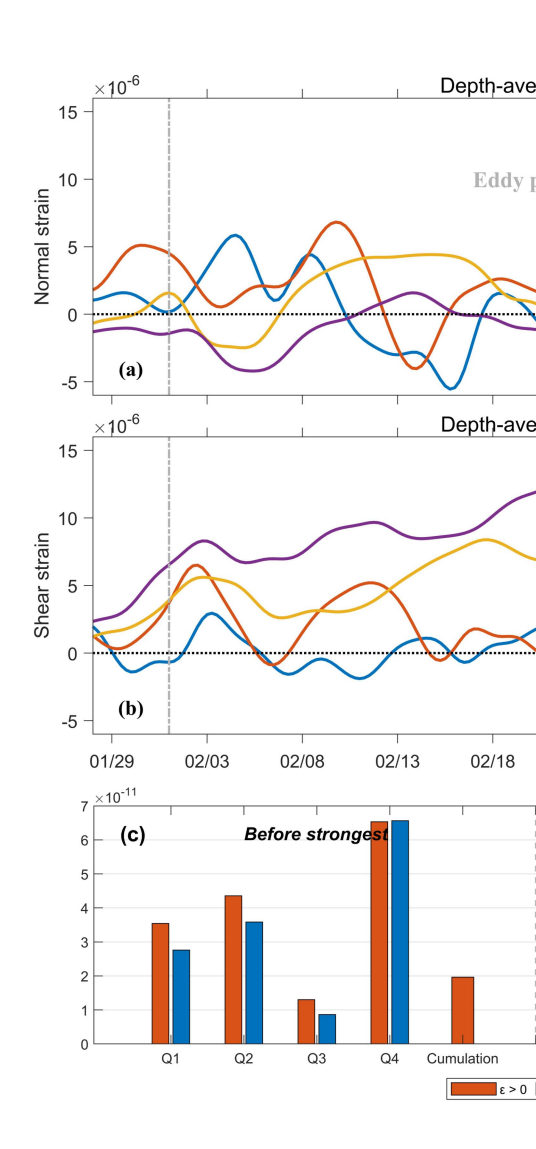


Figure 9: (a) Time series of depth-averaged (above 200 m) normal strain  $(-(\langle u_i u_i \rangle - \langle v_i v_i \rangle)) \frac{S_a}{2}$  of the CE for each mooring. (b) Time-series of depth-averaged (above 200 m) shear strain  $(-(u_i v_i \rangle S_s))$  of the CE for each mooring. (c) Time- (7 days) and depth-averaged (above 200 m) positive (red) and negative (blue) energy transfer rates before and after the NIKE reaching its peak at Q1-Q4. Cumulation bar represents sum of positive rates minus negative rates at Q1-Q4.

# **5 Conclusion**

During spring 2022, the CE passed through the northwestern SCS. Our four long-term moorings with ADCP instruments captured the interaction and energy exchange processes between eddy and local NIWs for the first time in this area. We found that NIWs can be largely enhanced by the passing CE. Horizontally, the CE transferred more energy to NIWs at the north side than that at the south side of the CE. This disparity may be attributed to the eddy asymmetry with stronger relative vorticity and shear in the northern region, which can significantly amplify NIWs generation (Zhao et al., 2021, 2023).

In vertical, the enhancement of NIKE occurred at above 200 m, with a maximum exceeding 12 J/m³ at



删除: (a) Time series of depth-averaged (above 200 m) normal strain of the CE for each mooring. (b) Time-series of depth-averaged (above 200 m) shear strain of the CE for each mooring.

删除

删除: Horizontally, the CE transferred more energy to NIWs at the north side than that at the south side of the CE due to asymmetry of eddy structure and strong shear.

260 a depth of 100 m. Power comparison of different NIWs modes during eddy period indicate that the CE 261 promoted percentage of first five modes, especially the second and third modes. Overall, NIWs drew 262 energy from the CE during the enhancing period of NIKE, while they gave energy back to the CE 263 during weakening period of NIKE. This study is helpful for understanding multi-scale interaction and 删除: us 264 energy cascade in the northwestern SCS. 删除: to understand 265 Data availability. The **CMEMS** available products are at 266 https://data.marine.copernicus.eu/product/GLOBAL MULTIYEAR PHY 001 030/services. The 267 ERA-5 wind data are available at <a href="https://doi.org/10.24381/cds.adbb2d47">https://doi.org/10.24381/cds.adbb2d47</a>. The WOA2018 268 climatological available monthly mean mixed layer depth data are at 269 https://www.ncei.noaa.gov/access/world-ocean-atlas-2018/. The AVISO eddy data are available at 270 https://www.aviso.altimetry.fr/en/data/products/value-added-products/global-mesoscale-eddytrajectory-product.html. The bathymetric data is from GEBCO Gridded Bathymetry Data 271 272 (https://download.gebco.net). The data used for plotting Figures for this paper is available at: 删除: mooring dataset 273 https://doi.org/10.5281/zenodo.14638959. 删除: are 删除: https://10.5281/zenodo.14638959. 274 Acknowledgments. This research is supported by Hainan Provincial Natural Science Foundation of 275 China (Grant No. 423RC547), the National Natural Science Foundation of China (Grant No. 42376023, 276 42176033), the Natural Science Foundation of Guangdong Province (Grant No. 2024A1515012218 and 277 2022A1515011736), the Innovational Fund for Scientific and Technological Personnel of Hainan 278 Province (Grant No. KJRC2023D39), and the Youth Innovation Promotion Association CAS (Grant No. 279 2022373). 280 Author Contribution. H.Z.X. and B.H. conceived the central idea. Q.A.C. and H.Z.X. conducted most 281 of the analyses and generated the Figures. Q.A.C., B.H. and H.Z.X. wrote the main manuscript. D.X.W, 282 C.L.L, Z.Y.Z., H.C.J. contributed to the revision of the manuscript. H.Z.X., Z.Y.Z., H.C.J., W.S., T.L., 283 L.W, S.M.L. and R.JC. conducted observations of the Mooring Array and participated in data analysis. 284 References 285 Alford, M. H.: Internal Swell Generation: The Spatial Distribution of Energy Flux from the Wind to

Mixed Layer Near-Inertial Motions, Journal of Physical Oceanography, 31, 2359-2368, 2001.

286

- 287 Alford, M. H.: Redistribution of energy available for ocean mixing by long-range propagation of
- 288 internal waves, Nature, 423, 159-162, 2003.
- 289 Alford, M. H.: Revisiting Near-Inertial Wind Work: Slab Models, Relative Stress, and Mixed Layer
- 290 Deepening, Journal of Physical Oceanography, 50, 3141-3156, 2020.
- 291 Alford, M. H., MacKinnon, J. A., Simmons, H. L., and Nash, J. D.: Near-Inertial Internal Gravity
- Waves in the Ocean, Annual Review of Marine Science, 8, 95-123, 2016.
- 293 Barkan, R., Srinivasan, K., Yang, L., McWilliams, J. C., Gula, J., and Vic, C.: Oceanic Mesoscale Eddy
- 294 Depletion Catalyzed by Internal Waves, Geophysical Research Letters, 48, e2021GL094376, 2021.
- 295 Chen, G., Hou, Y., and Chu, X.: Mesoscale eddies in the South China Sea: Mean properties,
- spatiotemporal variability, and impact on thermohaline structure, Journal of Geophysical Research, 116,
- 297 2011.
- 298 Chen, G., Xue, H., Wang, D., and Xie, Q.: Observed near-inertial kinetic energy in the northwestern
- 299 South China Sea, Journal of Geophysical Research: Oceans, 118, 4965-4977, 2013.
- 300 Chen, S., Chen, D., and Xing, J.: A study on some basic features of inertial oscillations and near-inertial
- 301 internal waves, Ocean Sci., 13, 829-836, 2017.
- 302 Chen, Z., Yu, F., Chen, Z., Wang, J., Nan, F., Ren, Q., Hu, Y., Cao, A., and Zheng, T.: Downward
- 303 Propagation and Trapping of Near-Inertial Waves by a Westward-Moving Anticyclonic Eddy in the
- 304 Subtropical Northwestern Pacific Ocean, Journal of Physical Oceanography, 53, 2105-2120, 2023.
- 305 Chu, F., Si, Z., Yan, X., Liu, Z., Yu, J., and Pang, C.: Physical structure and evolution of a cyclonic
- 306 eddy in the Northern South China sea, Deep Sea Research Part I: Oceanographic Research Papers, 189,
- 307 2022.
- 308 Chu, X., Xue, H., Qi, Y., Chen, G., Mao, Q., Wang, D., and Chai, F.: An exceptional anticyclonic eddy
- in the South China Sea in 2010, Journal of Geophysical Research: Oceans, 119, 881-897, 2014.
- 310 Dasaro, E. A.: The Energy Flux from the Wind to near-Inertial Motions in the Surface Mixed Layer,
- 311 Journal of Physical Oceanography, 15, 1043-1059, 1985.
- 312 Esposito, G., Donnet, S., Berta, M., Shcherbina, A. Y., Freilich, M., Centurioni, L., D'Asaro, E. A.,
- Farrar, J. T., Johnston, T. M. S., Mahadevan, A., Özgökmen, T., Pascual, A., Poulain, P.-M., Ruiz, S.,
- 314 Tarry, D. R., and Griffa, A.: Inertial Oscillations and Frontal Processes in an Alboran Sea Jet: Effects on
- 315 Divergence and Vertical Transport, Journal of Geophysical Research: Oceans, 128, e2022JC019004,
- 316 2023.
- 317 Fan, L., Sun, H., Yang, Q., and Li, J.: Numerical investigation of interaction between anticyclonic eddy
- and semidiurnal internal tide in the northeastern South China Sea, Ocean Science, 20, 241-264, 2024.
- 319 Ferrari, R. and Wunsch, C.: Ocean Circulation Kinetic Energy: Reservoirs, Sources, and Sinks, Annual
- 320 Review of Fluid Mechanics, 41, 253-282, 2009.
- Garrett, C.: What is the "near-inertial" band and why is it different from the rest of the internal wave
- 322 spectrum?, Journal of Physical Oceanography, 31, 962-971, 2001.
- 323 Guo, M., Chen, R., Xu, H., and Vetter, P. A.: Dynamical features of near-inertial motions in global
- 324 ocean based on the GDP dataset from 2000 to 2019, Acta Oceanologica Sinica, 40, 126-134, 2021.
- He, Q., Zhan, H., Cai, S., He, Y., Huang, G., and Zhan, W.: A New Assessment of Mesoscale Eddies in
- 326 the South China Sea: Surface Features, Three Dimensional Structures, and Thermohaline Transports,
- Journal of Geophysical Research: Oceans, 123, 4906-4929, 2018.
- 328 Huang, X., Wang, Z., Zhang, Z., Yang, Y., Zhou, C., Yang, Q., Zhao, W., and Tian, J.: Role of
- 329 Mesoscale Eddies in Modulating the Semidiurnal Internal Tide: Observation Results in the Northern
- 330 South China Sea, Journal of Physical Oceanography, 48, 1749-1770, 2018.

删除: Alford, M. H., Cronin, M. F., and Klymak, J. M.: Annual Cycle and Depth Penetration of Wind-Generated Near-Inertial Internal Waves at Ocean Station Papa in the Northeast Pacific, Journal of Physical Oceanography, 42, 889-909, 2012.

删除: Furuichi, N., Hibiya, T., and Niwa, Y.: Model-predicted distribution of wind-induced internal wave energy in the world's oceans, Journal of Geophysical Research: Oceans, 113, 2008.

- 331 Jing, Z., Chang, P., DiMarco, S. F., and Wu, L.: Observed Energy Exchange between Low-Frequency
- Flows and Internal Waves in the Gulf of Mexico, Journal of Physical Oceanography, 48, 995-1008,
- 333 2018.
- 334 Jing, Z., Wu, L., and Ma, X.: Energy Exchange between the Mesoscale Oceanic Eddies and Wind-
- Forced Near-Inertial Oscillations, Journal of Physical Oceanography, 47, 721-733, 2017.
- 336 Klein, P., Hua, B. L., and Carton, X.: Emergence of cyclonic structures due to the interaction between
- 337 near-inertial oscillations and mesoscale eddies, Quarterly Journal of the Royal Meteorological Society,
- 338 129, 2513-2525, 2003.
- 339 Kunze, E.: Near-Inertial Wave Propagation In Geostrophic Shear, Journal of Physical Oceanography,
- 340 15, 544-565, 1985.
- 341 Li, Q., Chen, Z., Guan, S., Yang, H., Jing, Z., Liu, Y., Sun, B., and Wu, L.: Enhanced Near-Inertial
- 342 Waves and Turbulent Diapycnal Mixing Observed in a Cold- and Warm-Core Eddy in the Kuroshio
- Extension Region, Journal of Physical Oceanography, 52, 1849-1866, 2022.
- Lin, P., Fang, W., Chen, Y., and Tang, X.: Temporal and spatial variation characteristics on eddies in the
- 345 South China Sea I. Statistical analyses, Acta Oceanologica Sinica, 29, 14-22, 2007.
- 346 Liu, G., Chen, Z., Lu, H., Liu, Z., Zhang, Q., He, Q., He, Y., Xu, J., Gong, Y., and Cai, S.: Energy
- 347 Transfer Between Mesoscale Eddies and Near Inertial Waves From Surface Drifter Observations,
- 348 Geophysical Research Letters, 50, 2023.
- 349 Liu, Y., Jing, Z., and Wu, L.: Wind Power on Oceanic Near-Inertial Oscillations in the Global Ocean
- 350 Estimated From Surface Drifters, Geophysical Research Letters, 46, 2647-2653, 2019.
- Nan, F., Xue, H., Xiu, P., Chai, F., Shi, M., and Guo, P.: Oceanic eddy formation and propagation
- 352 southwest of Taiwan, Journal of Geophysical Research: Oceans, 116, 2011.
- Oey, L. Y., Ezer, T., Wang, D. P., Fan, S. J., and Yin, X. Q.: Loop Current warming by Hurricane Wilma,
- 354 Geophysical Research Letters, 33, 2006.
- 355 Provenzale, A.: Transport by Coherent Barotropic Vortices, Annual Review of Fluid Mechanics, 31, 55-
- 356 93, 1999.
- 357 Thomas, J. and Daniel, D.: Turbulent exchanges between near-inertial waves and balanced flows,
- 358 Journal of Fluid Mechanics, 902, 2020.
- 359 Thomas, L. N.: On the modifications of near-inertial waves at fronts: implications for energy transfer
- 360 across scales, Ocean Dynamics, 67, 1335-1350, 2017.
- Wang, G., Chen, D., and Su, J.: Winter Eddy Genesis in the Eastern South China Sea due to Orographic
- Wind Jets, Journal of Physical Oceanography, 38, 726-732, 2008.
- 363 Wang, G., Su, J., and Chu, P. C.: Mesoscale eddies in the South China Sea observed with altimeter data,
- 364 Geophysical Research Letters, 30, 2003.
- Wang, X., Du, Y., Zhang, Y., Wang, T., Wang, M., and Jing, Z.: Subsurface Anticyclonic Eddy
- 366 Transited from Kuroshio Shedding Eddy in the Northern South China Sea, Journal of Physical
- 367 Oceanography, 53, 841-861, 2023.
- 368 Weller, R. A.: The Relation of Near-Inertial Motions Observed in the Mixed layer During the JASIN
- 369 (1978) Experiment to the Local Wind Stress and to the Quasi-Geostrophic Flow Field, Journal of
- 370 Physical Oceanography, 12, 1122-1136, 1982.
- 371 Xiu, P., Chai, F., Shi, L., Xue, H., and Chao, Y.: A census of eddy activities in the South China Sea
- during 1993–2007, Journal of Geophysical Research: Oceans, 115, 2010.
- 373 Xu, H., Zhang, Z., Vetter, P. A., Xie, Q., Long, T., and Hong, B.: Impact of Anticyclonic Eddy on
- 374 Nonlinear Wave Wave Interaction in the Southern South China Sea During Late Summer 2020,

- 375 Geophysical Research Letters, 49, 2022a.
- 376 Xu, X., Zhao, W., Huang, X., Hu, Q., Guan, S., Zhou, C., and Tian, J.: Observed Near-Inertial Waves
- 377 Trapped in a Propagating Anticyclonic Eddy, Journal of Physical Oceanography, 52, 2029-2047, 2022b.
- 378 Yu, X., Naveira Garabato, A. C., Vic, C., Gula, J., Savage, A. C., Wang, J., Waterhouse, A. F., and
- 379 MacKinnon, J. A.: Observed Equatorward Propagation and Chimney Effect of Near-Inertial Waves in
- 380 the Midlatitude Ocean, Geophysical Research Letters, 49, 2022.
- 381 Zhai, X., Johnson, H. L., and Marshall, D. P.: Significant sink of ocean-eddy energy near western
- boundaries, Nature Geoscience, 3, 608-612, 2010.
- Zhang, W. Z., Xue, H., Chai, F., and Ni, Q.: Dynamical processes within an anticyclonic eddy revealed
- from Argo floats, Geophysical Research Letters, 42, 2342-2350, 2015.
- 385 Zhang, Z., Liu, Y., Qiu, B., Luo, Y., Cai, W., Yuan, Q., Liu, Y., Zhang, H., Liu, H., Miao, M., Zhang, J.,
- 386 Zhao, W., and Tian, J.: Submesoscale inverse energy cascade enhances Southern Ocean eddy heat
- transport, Nature Communications, 14, 2023.
- Zhang, Z., Liu, Z., Richards, K., Shang, G., Zhao, W., Tian, J., Huang, X., and Zhou, C.: Elevated
- 389 Diapycnal Mixing by a Subthermocline Eddy in the Western Equatorial Pacific, Geophysical Research
- 390 Letters, 46, 2628-2636, 2019.
- 391 Zhang, Z., Tian, J., Qiu, B., Zhao, W., Chang, P., Wu, D., and Wan, X.: Observed 3D Structure,
- 392 Generation, and Dissipation of Oceanic Mesoscale Eddies in the South China Sea, Scientific Reports, 6,
- 393 2016.
- 394 Zhao, B., Liu, Z., Xu, Z., Yin, B., and Zheng, Q.: Spontaneous near-inertial wave generation from
- mesoscale eddy: Nonlinear forcing mechanism, Physics of Fluids, 35, 2023.
- 396 Zhao, B., Xu, Z., Li, Q., Min, W., Wang, Y., and Yin, B.: The characteristics of spontaneous near-
- 397 inertial wave generation from an anticyclonic mesoscale eddy, Journal of Oceanology and Limnology,
- 398 40, 413-427, 2021.

399

400

删除: Zhai, X., Greatbatch, R. J., Eden, C., and Hibiya, T.: On the Loss of Wind-Induced Near-Inertial Energy to Turbulent Mixing in the Upper Ocean, Journal of Physical Oceanography, 39, 3040-3045, 2009.